Supplementary Materials

Daily Global Sea Surface Ageostrophic Current Dataset from 1993–2023 via Physics-Informed Deep Learning

Guangxi Cui[1,2], Ka-Veng Yuen[3], Ying Chen[1,2], Zhiqiang Liu[4], Dingqi Yang[5], Guanliang Liu[6,7], Zhongya Cai[1,2*]

[1]State Key Laboratory of Internet of Things for Smart City, Department of Ocean Science and Technology, University of Macau, Macau, China

[2]Center for Ocean Research in Hong Kong and Macau (CORE), Hong Kong, China

[3]State Key Laboratory of Internet of Things for Smart City, Department of Civil and Environmental Engineering, University of Macau, Macau, China

[4]Department of Ocean Science and Engineering and Center for Complex Flows and Soft Matter Research, Southern University of Science and Technology, Shenzhen, China

[5]State Key Laboratory of Internet of Things for Smart City, Department of Computer and Information Science, University of Macau, Macau, China

[6]State Key Laboratory of Physical Oceanography, Institute of Oceanographic Instrumentation, Shandong Academy of Sciences, Jinan, China

[7]Qilu University of Technology (Shandong Academy of Sciences), Jinan, China

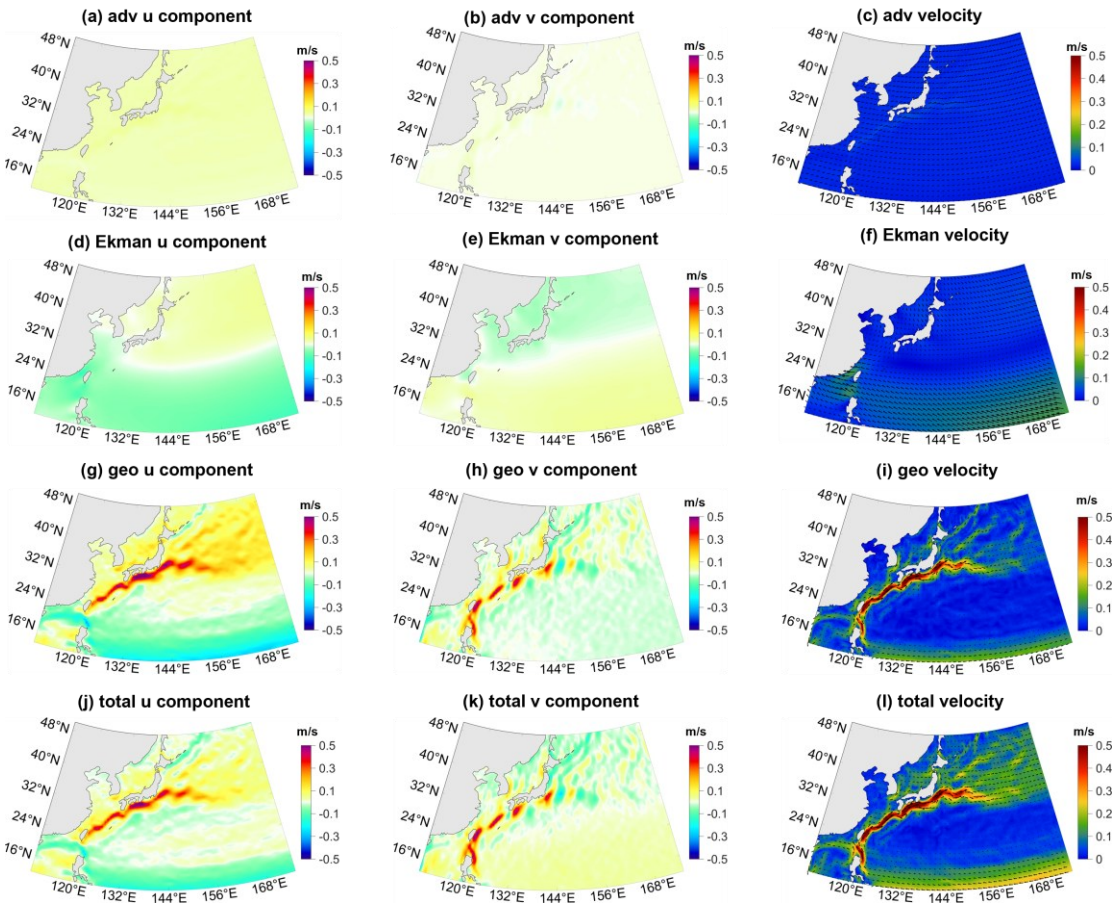

Figure S1: Results of sea surface circulation correction for the Kuroshio Current from 1993 to 2023, using the AC-PIDNN model. Panels (a)–(c) show the u-component, v-component, and flow field of the advective component; panels (d)–(f) show the u-component, v-component, and flow field of the Ekman component; panels (g)–(i) show the u-component, v-component, and flow field of the geostrophic component; panels (j)–(l) show the u-component, v-component, and flow field of the total circulation.

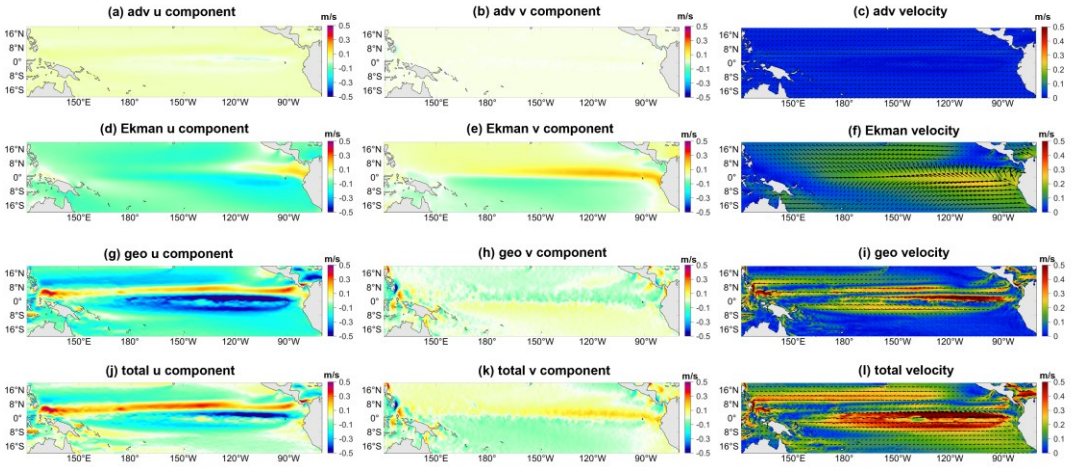

Figure S2: Results of sea surface circulation correction for the Equatorial Region from 1993 to 2023, using the AC-PIDNN model. Panels (a)–(c) show the u-component, v-component, and flow field of the advective component; panels (d)–(f) show the u-component, v-component, and flow field of the Ekman component; panels (g)–(i) show the u-component, v-component, and flow field of the geostrophic component; panels (j)–(l) show the u-component, v-component, and flow field of the total circulation.

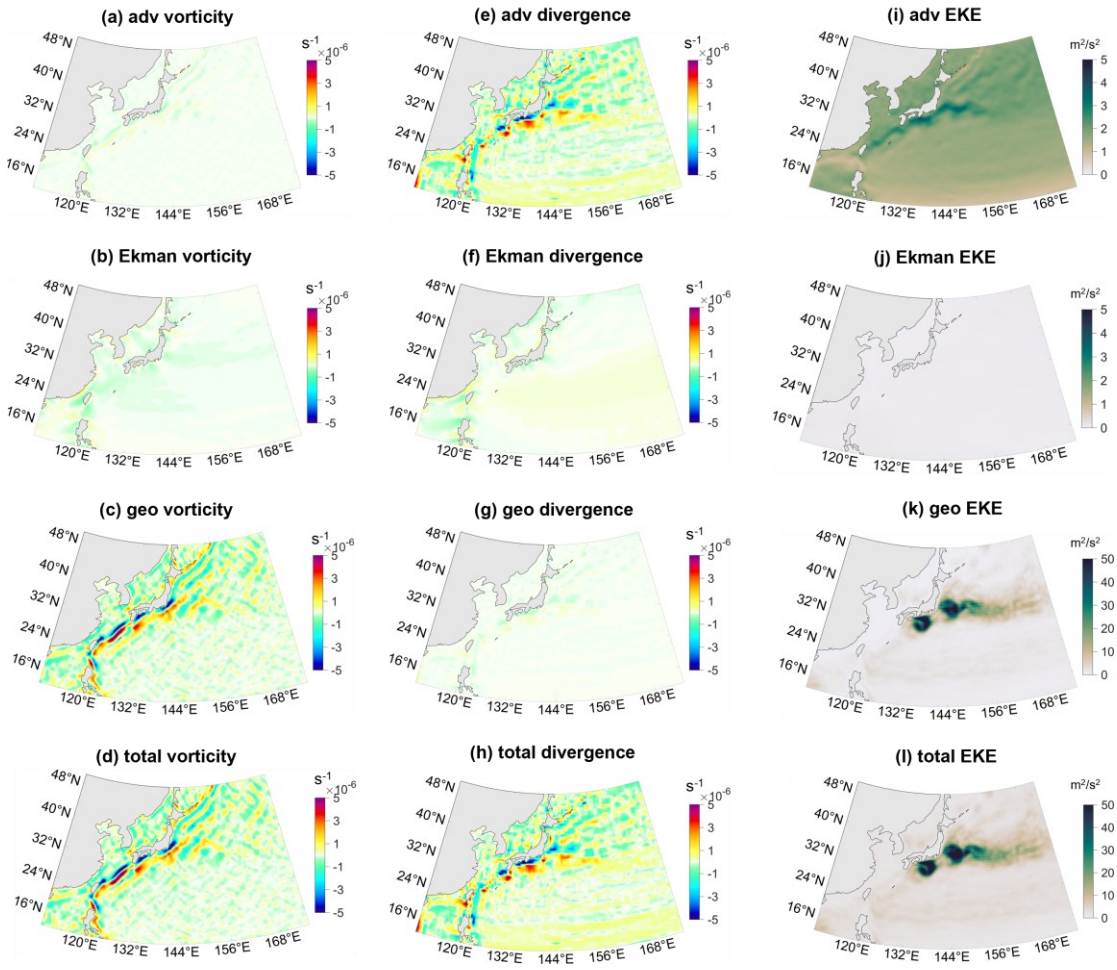

Figure S3: Characteristics of the dynamic parameters of the corrected 30-year average sea surface circulation in the Kuroshio Current. Panels (a)–(d) showing the vorticity of the advective, Ekman, geostrophic, and total components, respectively; panels (e)–(h) showing the divergence of the advective, Ekman, geostrophic, and total components, respectively; panels (i)–(l) showing the eddy kinetic energy (EKE) of the advective, Ekman, geostrophic, and total components, respectively.

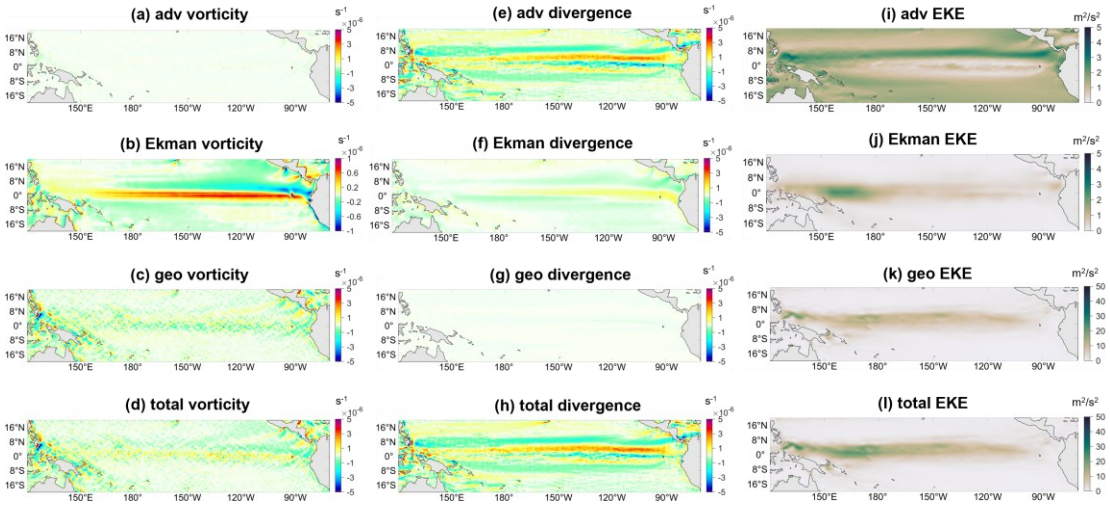

Figure S4: Characteristics of the dynamic parameters of the corrected 30-year average sea surface circulation in the Equatorial Region. Panels (a)–(d) showing the vorticity of the advective, Ekman, geostrophic, and total components, respectively; panels (e)–(h) showing the divergence of the advective, Ekman, geostrophic, and total components, respectively; panels (i)–(l) showing the eddy kinetic energy (EKE) of the advective, Ekman, geostrophic, and total components, respectively.